Open Access
Published Online First: September 2021

Baghdad Science Journal
2022, 19(2): 321-328

P-ISSN: 2078-8665
E-ISSN: 2411-7986

DOI: http://dx.doi.org/10.21123/bsj.2022.19.2.0321

Numerical Solutions of Two-Dimensional Vorticity Transport Equation Using Crank-Nicolson Method

***Maan A. Rasheed*[1]* ***Suad Naji Kadhim*[2]*

[1]Department of Mathematics, College of Basic Education, Mustansiriyah University, Baghdad, Iraq
[2]Department of Mathematics, College of Science, University of Baghdad, Baghdad, Iraq
Corresponding Author: maan.rasheed.edbs@uomustansiriyah.edu.iq, suad.n@sc.uobaghdad.edu.iq
ORCID ID: https://orcid.org/0000-0002-7955-1424*, https://orcid.org/0000-0003-0229-1481

Received 18/11/2020, Accepted 22/12/2020, Published Online First 20/9/2021, Published 1/4/2022

Abstract:

This paper is concerned with the numerical solutions of the vorticity transport equation (VTE) in two-dimensional space with homogenous Dirichlet boundary conditions. Namely, for this problem, the Crank-Nicolson finite difference equation is derived. In addition, the consistency and stability of the Crank-Nicolson method are studied. Moreover, a numerical experiment is considered to study the convergence of the Crank-Nicolson scheme and to visualize the discrete graphs for the vorticity and stream functions. The analytical result shows that the proposed scheme is consistent, whereas the numerical results show that the solutions are stable with small space-steps and at any time levels.

Keywords: Finite difference, Reynolds number, Stream function, Truncation error, Vorticity function.

Introduction:

This work is concerned with the two-dimensional vorticity-transport-equation (VTE), which is a nonlinear time-dependent partial differential equation:

$$\frac{\partial \omega}{\partial t} = \frac{1}{R}\left(\frac{\partial^2 \omega}{\partial x^2} + \frac{\partial^2 \omega}{\partial y^2}\right) - \left(\frac{\partial \psi}{\partial y}\right)\left(\frac{\partial \omega}{\partial x}\right) + \left(\frac{\partial \psi}{\partial x}\right)\left(\frac{\partial \omega}{\partial y}\right), \quad (1)$$

$$\omega = -\left(\frac{\partial^2 \psi}{\partial x^2} + \frac{\partial^2 \psi}{\partial y^2}\right), \quad (2)$$

for $(x, y) \in D, t > 0$,

with the following initial and boundary conditions:

$$\omega(x, y, 0) = \omega_0(x, y), \quad \psi(x, y, 0) = \psi_0(x, y), \quad (3)$$
$$(x, y) \in D, t > 0,$$

$$\omega(x, y, t) = \psi(x, y, t) = 0, \quad (4)$$
$$(x, y) \in \partial D \quad, t > 0,$$

where ω refers to the vorticity function, and ψ refers to the stream function, and $R > 0$ is the Reynolds number; $D = \{(x, y): a < x < b;\ a < y < b\}$; and $\partial D = \{(a, y), (b, y), (x, a), (x, b)\}$; and ω_0, ψ_0 are smooth nonnegative functions satisfying equation (2).

Due to the various applications of time-dependent partial differential equations in various fields of science, since last century, many authors have been interested in studying the analytical and numerical solutions of such types of problems including linear equations, nonlinear equations, partial integro-differential equations, and time-space fractional-order partial differential equations, see for instance [1-5]. In fluid dynamics, the numerical solutions of various Mathematical models, including problem (1)-(2), have been studied by some authors, see for instance [6,7].

It is known that problem (1)-(2) is used to study the unsteady flow problem in two-dimensional space. In other words, it can be used for solving the two-dimensional viscous incompressible flow. In addition, the two-dimensional vorticity transport equation can be used in some applications, such as analysis of laminar to turbulent flow transition, studies on free and mixed convection and the modeling of turbulent flows. For more details about the importance, derivation and the applications of this problem, see [8,9].

In fact, this problem cannot be solved analytically due to the nonlinear terms that appear in equation (1). So that since the last decades, problem (1)-(2), with different initial-boundary conditions, has been solved numerically by some authors using several methods, such as the Petrov-Galerkin finite element method [10], finite difference schemes, see for instance [11-16], and the boundary-domain integral method [17]. Because of the poor stability properties of explicit finite difference methods, the implicit methods are more recommended to compute the numerical solutions of initial-boundary value problems in two or more dimensions-space. The Crank-Nicolson method is one of the most recommended implicit methods for solving many types of second order linear problems with constant coefficients due to its high order of convergence and unconditional stability. However, it is not always guaranteed that Crank- Nicolson method is stable and applicable for other types of problems such as nonlinear problems, problems with variable coefficients and problems with nonlinear boundary conditions. In this work, the Crank-Nicolson finite difference scheme is used to solve problem (1)-(4). Moreover, it is shown that the proposed scheme is consistent and stable.

This paper is divided into seven sections. In the second section, the discrete formulas of equations (1) and (2), using Crank-Nicolson scheme, are derived. In the third section, the matrix forms of the Crank-Nicolson finite difference equations are presented. The consistency of the discrete difference equations is studied in the fourth section. In the fifth section, the stability condition for the matrices form is discussed. In the sixth section, the Crank-Nicolson discrete scheme is used to compute the numerical solutions of problem (1)-(4) with a certain initial function and a fixed value to the Reynolds number. Moreover, the numerical simulations for the vorticity and stream functions are shown in two-dimensional spaces and at different time levels. Finally, some conclusions and future works are stated in the seventh section.

The Discrete Problem

For convenient computations, let h refers to the space-step in x and y directions. In addition, let k refers to the time-step, such that:

$$x_0 = a, \quad x_i = x_0 + ih, \quad x_m = b,$$
$$y_0 = a, \quad y_i = y_0 + jh, \quad y_m = b,$$
$$\text{for } h = (b-a)/m \ ; \quad i,j = 1,2,3,\dots m-1,$$
$$\text{and } t_n = nk \ , \text{ for } k > 0 \ ; \quad n = 0,1,2,\dots.$$

Consider that $\omega_{i,j}^n$ and $\psi_{i,j}^n$ are the approximate values to $\omega(x_i, y_j, t_n)$ and $\psi(x_i, y_j, t_n)$, respectively.

In addition, the discrete-space $D_{i,j}^n$, is defined as follows:

$$D_{i,j}^n = \{ (x_i, y_j, t_n);\ i,j = 0,1,2 \dots m\,;\, n \geq 0 \}$$

Taking Taylor expansion to $\omega(x, y, (n+1)k)$ about $\omega(x, y, nk)$, it follows:

$$\omega(x,y,(n+1)k) = \left(1 + k\frac{\partial}{\partial t} + \frac{k^2}{2}\frac{\partial^2}{\partial t^2} + \cdots\right)\omega(x,y,nk).$$

This implies that

$$\omega(x,y,(n+1)k) = \exp(k\frac{\partial}{\partial t})\omega(x,y,nk) \quad (5)$$

The last equation can be rewritten as follows:

$$\exp\left(-\frac{k}{2}\frac{\partial}{\partial t}\right)\omega(x,y,(n+1)k) = \exp\left(\frac{k}{2}\frac{\partial}{\partial t}\right)\omega(x,y,nk)$$

By equation (1), the last equation becomes:

$$\exp\left(-\frac{k}{2}[\frac{1}{R}\left(\frac{\partial^2}{x^2} + \frac{\partial^2}{y^2}\right) - \frac{\partial\psi}{\partial y}\frac{\partial}{\partial x} + \frac{\partial\psi}{\partial x}\frac{\partial}{\partial y}]\right)\omega(x,y,(n+1)k) = \exp\left(\frac{k}{2}[\frac{1}{R}\left(\frac{\partial^2}{x^2} + \frac{\partial^2}{y^2}\right) - \frac{\partial\psi}{\partial y}\frac{\partial}{\partial x} + \frac{\partial\psi}{\partial x}\frac{\partial}{\partial y}]\right)\omega(x,y,nk)$$

Next, the partial derivatives ω_x, ψ_x, ω_y and ψ_y are approximated by the first-order central finite difference operators, δ_x, δ_y, and the partial derivatives, ω_{xx}, ω_{yy} are approximated by the second-order central finite difference operators, ${\delta^2}_x, {\delta^2}_y$, respectively, and ω, ψ, are replaced by $\omega_{i,j}^n$, $\psi_{i,j}^n$, respectively, then the above equation becomes:

$$\exp\left(-\frac{k}{2}\left[\frac{1}{R}\left(\frac{{\delta^2}_x}{h^2} + \frac{{\delta^2}_y}{h^2}\right) - \left(\frac{\delta_y\psi_{i,j}^n}{2h}\right)\left(\frac{\delta_x}{2h}\right) + \left(\frac{\delta_x\psi_{i,j}^n}{2h}\right)\left(\frac{\delta_y}{2h}\right)\right]\right)\omega_{i,j}^{n+1} = \exp\left(\frac{k}{2}\left[\frac{1}{R}\left(\frac{{\delta^2}_x}{h^2} + \frac{{\delta^2}_y}{h^2}\right) - \left(\frac{\delta_y\psi_{i,j}^n}{2h}\right)\left(\frac{\delta_x}{2h}\right) + \left(\frac{\delta_x\psi_{i,j}^n}{2h}\right)\left(\frac{\delta_y}{2h}\right)\right]\right)\omega_{i,j}^n$$

For simplicity, the last equation can be rewritten as follows:

$$\exp\left(-\frac{r}{2R}({\delta^2}_x + {\delta^2}_y) + \frac{r}{8}(\delta_y\psi_{i,j}^n)(\delta_x) - \frac{r}{8}(\delta_x\psi_{i,j}^n)(\delta_y)\right)\omega_{i,j}^{n+1} = \exp\left(\frac{r}{2R}({\delta^2}_x + {\delta^2}_y) - \frac{r}{8}(\delta_y\psi_{i,j}^n)(\delta_x) + \frac{r}{8}(\delta_x\psi_{i,j}^n)(\delta_y)\right)\omega_{i,j}^n,$$

where $r = k/h^2$.

Taking the Taylor expansion for each side in the above equation, and truncating after second terms yield that:

$$\left(1 - \frac{r}{2R}({\delta^2}_x + {\delta^2}_y) + \frac{r}{8}(\delta_y\psi_{i,j}^n)(\delta_x) - \frac{r}{8}(\delta_x\psi_{i,j}^n)(\delta_y)\right)\omega_{i,j}^{n+1} =$$

$$\left(1+\frac{r}{2R}\left(\delta^2{}_x+\delta^2{}_y\right)-\frac{r}{8}\left(\delta_y\psi^n_{i,j}\right)(\delta_x)+\frac{r}{8}\left(\delta_x\psi^n_{i,j}\right)(\delta_y)\right)\omega^n_{i,j} \qquad (6)$$

$i,j=1,2,3,\ldots..m-1;\quad n=0,1,2,\ldots.$

Next, the spatial derivatives in equation (2) are approximated by the central finite difference operator of second order as follows:

$$\omega^n_{i,j}=-\left(\frac{\delta^2{}_x\psi^n_{i,j}}{h^2}+\frac{\delta^2{}_y\psi^n_{i,j}}{h^2}\right) \qquad (7)$$

For simplicity, equations (6) and (7) can be rewritten as follows:

$$\begin{aligned}
&\left(1+\frac{2r}{R}\right)\omega^{n+1}_{i,j}-\frac{r}{2R}\left(\omega^{n+1}_{i+1,j}+\omega^{n+1}_{i-1,j}+\omega^{n+1}_{i,j+1}+\omega^{n+1}_{i,j-1}\right)\\
&\quad+\frac{r}{8}\left(\psi^n_{i,j+1}-\psi^n_{i,j-1}\right)\left(\omega^{n+1}_{i+1,j}-\omega^{n+1}_{i-1,j}\right)\\
&\quad-\frac{r}{8}\left(\psi^n_{i+1,j}-\psi^n_{i-1,j}\right)\left(\omega^{n+1}_{i,j+1}-\omega^{n+1}_{i,j-1}\right)\\
&=\left(1-\frac{2r}{R}\right)\omega^n_{i,j}+\frac{r}{2R}\left(\omega^n_{i+1,j}+\omega^n_{i-1,j}+\omega^n_{i,j+1}+\omega^n_{i,j-1}\right)\\
&\quad-\frac{r}{8}\left(\psi^n_{i,j+1}-\psi^n_{i,j-1}\right)\left(\omega^n_{i+1,j}-\omega^n_{i-1,j}\right)\\
&\quad+\frac{r}{8}\left(\psi^n_{i+1,j}-\psi^n_{i-1,j}\right)\left(\omega^n_{i,j+1}-\omega^n_{i,j-1}\right),
\end{aligned}$$

and

$$-h^2\omega^n_{i,j}=\psi^n_{i+1,j}+\psi^n_{i-1,j}+\psi^n_{i,j+1}+\psi^n_{i,j-1}-4\psi^n_{i,j}\ ,$$

$i,j=1,2,3,\ldots..m-1;\quad n=0,1,2,\ldots.$

Finally, in the discrete space, $D^n_{i,j}$, the initial-boundary conditions (3) and (4) become:

$\omega^0_{i,j}=\omega_0(x_i,y_i),\quad \psi^0_{i,j}=\psi_0(x_i,y_i),$ (8)

$i,j=0,1,2,\ldots\ldots.m$

$\omega^n_{0,j}=\omega^n_{m,j}=\omega^n_{i,0}=\omega^n_{i,m}=0\ ,$ (9)

$\psi^n_{0,j}=\psi^n_{m,j}=\psi^n_{i,0}=\psi^n_{i,m}=0,$ (10)

$i,j=1,2,3,\ldots\ldots.m-1\ ,\ n>0$

The Matrix Form

The difference equations (6) and (7) of Crank-Nicolson method can be presented in matrix form as follows:

$$\left(I-\frac{r}{2R}C+\frac{r}{8}\,V^n_2A-\frac{r}{8}\,V^n_1B\right)\omega^{n+1}=\left(I+\frac{r}{2R}C-\frac{r}{8}\,V^n_2A+\frac{r}{8}\,V^n_1B\right)\omega^n,\qquad (11)$$

$$-h^2\omega^n=C\psi^n\ ,\qquad n=0,1,2,\ldots.\qquad (12)$$

$$\text{where}\quad V^n_1=A\psi^n\ ,V^n_2=B\psi^n,\qquad (13)$$

$$\omega^n=\left(\omega^n_{1,1},\omega^n_{2,1},\ldots,\omega^n_{m-1,1};\ \omega^n_{1,2},\omega^n_{2,2},\ldots,\omega^n_{m-1,2};\ldots.;\omega^n_{1,m-1},\omega^n_{2,m-1},\ldots,\omega^n_{m-1,m-1}\right)\ ,\quad (14)$$

$$\psi^n=\left(\psi^n_{1,1},\psi^n_{2,1},\ldots,\psi^n_{m-1,1}\ ;\ \psi^n_{1,2},w^n_{2,2},\ldots,\psi^n_{m-1,2};\ldots.;\psi^n_{1,m-1},\psi^n_{2,m-1},\ldots,\psi^n_{m-1,m-1}\right),\quad (15)$$

M_1,M_2,A and B take the following forms:

$$A=\begin{bmatrix}0 & I_1 & & 0\\ -I_1 & 0 & I_1 & \\ & & \ddots & \\ 0 & & -I_1 & 0\end{bmatrix}_{(m-1)^2\times(m-1)^2}$$

$$B=\begin{bmatrix}B_1 & & 0\\ & B_1 & \\ & & \ddots\\ 0 & & B_1\end{bmatrix}_{(m-1)^2\times(m-1)^2},$$

$$B_1=\begin{bmatrix}0 & 1 & & 0\\ -1 & 0 & 1 & \\ & & \ddots & \\ 0 & & -1 & 0\end{bmatrix}_{(m-1)\times(m-1)}$$

$$C=\begin{bmatrix}C_1 & I_1 & & 0\\ I_1 & C_1 & I_1 & \\ & & \ddots & \\ 0 & & I_1 & C_1\end{bmatrix}_{(m-1)^2\times(m-1)^2},$$

$$C_1=\begin{bmatrix}-4 & 1 & & 0\\ 1 & -4 & 1 & \\ & & \ddots & \\ 0 & & 1 & -4\end{bmatrix}_{(m-1)\times(m-1)},$$

and I,I_1 are the identity matrices of order $(m-1)^2$, $(m-1)$, respectively.

Remark 1 At each advance time level $(n+1)$, to find the numerical solution of problem (1)-(4) using Crank-Nicolson discrete scheme (6) and (7), the following procedure is applied:

- Solve the linear system (12), to compute the vector ψ^n .
- By (13), find the vectors V^n_1 , V^n_2 .
- Substitute V^n_1 , V^n_2 in (11) and solve the resulting linear system (11), to obtain the solution ω^{n+1} .

Consistency of the Discrete Problem

In this section, the local truncation errors (consistency errors) of the Crank-Nicolson discrete difference equations are estimated. In addition, the orders of accuracy are shown.

Theorem 1 Let $T^n_{i,j}$ and $\hat{T}^n_{i,j}$ be the local-truncation-errors, at a mesh point $\left(x_i,y_j,t_n\right)$, of the discrete equations (6) and (7), respectively. There are positive constants C_1,C_2,C_3, such that:

$$|T^n_{i,j}|\le C_1k^2+C_2kh^2\quad ,\quad |\,\hat{T}^n_{i,j}|\le C_3h^2.$$

Proof: Set $\omega|^n_{i,j}=\omega\left(x_i,y_j,t_n\right),$

$\psi|^n_{i,j}=\psi\left(x_i,y_j,t_n\right),$

By the Crank-Nicolson difference equation (6), it follows that

$$T_{i,j}^n = \begin{pmatrix} 1-\frac{r}{2R}\left(\delta^2{}_x+\delta^2{}_y\right) \\ +\frac{r}{8}\left(\delta_y\psi|_{i,j}^n\right)(\delta_x)-\frac{r}{8}\left(\delta_x\psi|_{i,j}^n\right)(\delta_y) \end{pmatrix}\omega|_{i,j}^{n+1}$$
$$-\left(1+\frac{r}{2R}\left(\delta^2{}_x+\delta^2{}_y\right)-\frac{r}{8}\left(\delta_y\psi|_{i,j}^n\right)(\delta_x)\right.$$
$$\left.+\frac{r}{8}\left(\delta_x\psi|_{i,j}^n\right)(\delta_y)\right)\omega|_{i,j}^n$$

Since $\omega|_{i,j}^{n+1}=\exp(k\frac{\partial}{\partial t})\omega|_{i,j}^n$

By truncating after the second term, it yields that

$$\omega|_{i,j}^{n+1}=\left(1+k\frac{\partial}{\partial t}+k^2\frac{\partial^2}{\partial t^2}\right)\omega|_{i,j}^n$$

Thus

$$T_{i,j}^n=(\omega|_{i,j}^{n+1}-\omega|_{i,j}^n)+$$
$$\left[\frac{-r}{2R}\left(\delta^2{}_x\omega|_{i,j}^n+\delta^2{}_y\omega|_{i,j}^n\right)+\frac{r}{8}\left(\delta_y\psi|_{i,j}^n\right)\left(\delta_x\omega|_{i,j}^n\right)\right.$$
$$\left.-\frac{r}{8}\left(\delta_x\psi|_{i,j}^n\right)\left(\delta_y\omega|_{i,j}^n\right)\right]\left[2+k\frac{\partial}{\partial t}\right.$$
$$\left.+k^2\frac{\partial^2}{\partial t^2}\right]$$

Truncating the Taylor expansion in the above equation yields that

$$T_{i,j}^n=k\left(\frac{\partial\omega}{\partial t}|_{i,j}^n+\frac{k}{2}\frac{\partial^2\omega}{\partial t^2}+O(k^2)\right)$$
$$+\left[\frac{-k}{2R}\left[\left(\frac{\partial^2\omega}{\partial x^2}+\frac{\partial^2\omega}{\partial y^2}\right)|_{i,j}^n+O(h^2)\right]\right.$$
$$+\frac{k}{2}\left[\frac{\partial\psi}{\partial y}|_{i,j}^n+O(h^2)\right]\left[\frac{\partial\omega}{\partial x}|_{i,j}^n\right.$$
$$\left.+O(h^2)\right]$$
$$-\frac{k}{2}\left[\frac{\partial\psi}{\partial x}|_{i,j}^n+O(h^2)\right]\left[\frac{\partial\omega}{\partial y}|_{i,j}^n\right.$$
$$\left.\left.+O(h^2)\right]\right]\left[2+k\frac{\partial}{\partial t}+k^2\frac{\partial^2}{\partial t^2}\right]$$

By equation (1), it yields that

$$\left[\frac{\partial\omega}{\partial t}-\frac{1}{R}\left(\frac{\partial^2\omega}{\partial x^2}+\frac{\partial^2\omega}{\partial y^2}\right)+\left(\frac{\partial\psi}{\partial y}\right)\left(\frac{\partial\omega}{\partial x}\right)\right.$$
$$\left.-\left(\frac{\partial\psi}{\partial x}\right)\left(\frac{\partial\omega}{\partial y}\right)\right]|_{i,j}^n=0$$

Thus

$T_{i,j}^n=O(k^2)+O(kh^2)$,

or $\qquad T_{i,j}^n=O(k^2+kh^2)$

By assuming that, in the domain $D_{i,j}^n$, all partial derivatives of ω,ψ are bounded, there are positive constants $C_1, C_2\in R$ such that

$$|T_{i,j}^n|\le C_1k^2+C_2kh^2$$

For the difference equation (7), the local truncation error at the mesh point(x_i,y_j,t_n), takes the form:

$$\hat{T}_{i,j}^n=\omega|_{i,j}^n+\left(\frac{\delta^2{}_x\psi|_{i,j}^n}{h^2}+\frac{\delta^2{}_y\psi|_{i,j}^n}{h^2}\right)$$

Truncating the Taylor expansion in the above equation yields that

$$\hat{T}_{i,j}^n=\omega|_{i,j}^n+\left(\frac{\partial^2\psi}{\partial x^2}+\frac{\partial^2\psi}{\partial y^2}\right)|_{i,j}^n+O(h^2)$$

By equation (2), it yields that

$$\omega|_{i,j}^n+\left(\frac{\partial^2\psi}{\partial x^2}+\frac{\partial^2\psi}{\partial y^2}\right)|_{i,j}^n=0\ .$$

So, $\hat{T}_{i,j}^n=O(h^2)$, this implies that there is $C_3>0$ such that

$$|\hat{T}_{i,j}^n|\le C_3h^2$$

Definition 1 [18] A difference equation of a parabolic equation is called consistent, if the following condition is satisfied:

$$\frac{LTE}{k}\ \to 0,\quad \text{as}\quad h,k\to 0$$

Based on Definition 1 and Theorem 1, the following theorem can be proved.

Theorem 2 The difference equation of Crank-Nicolson scheme (6) and (7) is consistent.

Stability of the Discrete Problem

In this section, the stability for the matrix form (11) and (12) are discussed.

The matrix form Crank-Nicolson scheme (11) and (12) can be rewritten as follows:

$$\omega^{n+1}=H_n\,\omega^n\ ,\ \forall\, n\ , \qquad (16)$$

where

$$H_n=\left(I-\frac{r}{2R}C+\frac{r}{8}\,V_2^nA-\frac{r}{8}\,V_1^nB\right)^{-1}\left(I+\frac{r}{2R}C-\frac{r}{8}\,V_2^nA+\frac{r}{8}\,V_1^nB\right).$$

Theorem 3 Based on a constant time-step, the necessary and sufficient condition for stability of the matrix form (16) of the Crank-Nicolson scheme is

$\|H_n\|\le 1$, for all n. (17)

where $\|H_n\|_2=max_s|\lambda_s|$, (18)

$\lambda_s(s=1,2,\dots,(m-1)^2)$ are the eigenvalues of H_n .

Proof: This theorem can be proved easily following the same technique used in [18].

Numerical Experiment

The Crank-Nicolson difference equations (6) and (7) are used in this section to find the numerical solution of problem (1)-(4), with $R=1$, and the following initial function:

$\omega_0(x,y)=(1-x^2)(1-y^2),\quad -1\le x\le 1,$
$-1\le y\le 1$ (19)

Moreover, in order to study the numerical convergence, different space-steps $(h=0.4,0.2,0.1)$ and a small fixed time-step $k=0.002$ are considered in the computations.

Based on the type of the initial function (19), the solution of problem (1)-(4) with (19) is symmetric and positive. Therefore, it is sufficient to find only the first M components of the numerical solution vectors, ω^n, ψ^n , at each time level.

where $M = \begin{cases} \frac{(m-1)^2}{2} & if \quad m \text{ is even} \\ \frac{(m-1)^2+1}{2} & if \quad m \text{ is odd} \end{cases}$

In addition, for each of $h = 0.4, h = 0.2$, and at the time level n, the errors bounds will be computed that show, at some fixed meshes-points, the differences between the numerical solutions (ω_h^n, ψ_h^n) and $(\omega_{h/2}^n, \psi_{h/2}^n)$ with respect to h and $h/2$, respectively, as follows:

$$\begin{cases} E_h^n(\omega) = \frac{\sum_{(x,y)\in\pi}\left|\omega_h^n(x,y) - \omega_{h/2}^n(x,y)\right|}{N=8} \\ E_h^n(\psi) = \frac{\sum_{(x,y)\in\pi}\left|\psi_h^n(x,y) - \psi_{h/2}^n(x,y)\right|}{N=8} \end{cases} \quad (20)$$

where $\pi = \{(x,y), s.t.\ x = -1 + ih\ ; y = -1 + jh\ ;\ i = 1,2,3,4\ ; j = 1,2\ ; h = 0.4\}$.

Results and Discussions:
Numerical:

The numerical results are presented in the next tables, where Matlab software is used in the computational processes. In Tables 1, 2 and 3, the numerical results are shown, for $h = 0.4, 0.2, 0.1$, at the time-levels 100, 200 and 400, respectively. In Table 4, the formula (20) is used to compute the errors bounds of numerical solutions, for $h = 0.4, 0.2$, at time-levels: $n = 100, 200, 400$. In table 5, the numerical values of the norm $\|H_n\|_2$, defined in (18), are shown, for $h = 0.4, 0.2, 0.1$, at time-levels: $n = 100, 200$ and 400.

From Tables 1-3, it is observed that the numerical values for vorticity and stream are decreasing as time level increases. In addition, Table 4 shows that at a fixed time level, the corresponding error bounds decrease, as the space grids are refined. This indicates that the numerical solution is convergent. On the other hand, at any fixed space-step, the corresponding errors decrease as time increases. Moreover, Table 5 shows that the numerical results are stable (condition (17) is satisfied) with any space-step and time level.

Table 1. Numerical solutions (ω, ψ), $n = 100$ $(t = 0.2)$

h	0.1		0.2		0.4	
(x,y)	ω	ψ	ω	ψ	ω	ψ
(-0.6,-0.6)	0.1364	0.0279	0.1373	0.0282	0.1413	0.0297
(-0.2,-0.6)	0.2209	0.0451	0.2223	0.0457	0.2282	0.0480
(0.2,-0.6)	0.2200	0.0451	0.2215	0.0456	0.2271	0.0479
(0.6,-0.6)	0.1349	0.0278	0.1360	0.0282	0.1396	0.0296
(-0.6,-0.2)	0.2191	0.0450	0.2204	0.0456	0.2262	0.0479
(-0.2,-0.2)	0.3561	0.0729	0.3583	0.0739	0.3667	0.0775
(0.2,-0.2)	0.3556	0.0729	0.3578	0.0738	0.3660	0.0775
(0.6,-0.2)	0.2182	0.0450	0.2198	0.0456	0.2252	0.0478

Table 2. Numerical solutions (ω, ψ), $n = 200$ $(t = 0.4)$

h	0.1		0.2		0.4	
(x,y)	ω	ψ	ω	ψ	ω	ψ
(-0.6,-0.6)	0.0505	0.0104	0.0512	0.0106	0.0538	0.0114
(-0.2,-0.6)	0.0819	0.0168	0.0829	0.0171	0.0871	0.0184
(0.2,-0.6)	0.0817	0.0168	0.0828	0.0171	0.0869	0.0184
(0.6,-0.6)	0.0503	0.0103	0.0510	0.0105	0.0535	0.0113
(-0.6,-0.2)	0.0816	0.0168	0.0826	0.0171	0.0867	0.0184
(-0.2,-0.2)	0.1323	0.0271	0.1340	0.0276	0.1407	0.0297
(0.2,-0.2)	0.1322	0.0271	0.1339	0.0276	0.1406	0.0297
(0.6,-0.2)	0.0814	0.0167	0.0825	0.0171	0.0866	0.0184

Table 3. Numerical solutions (ω, ψ), $n = 400$ $(t = 0.8)$

h	0.1		0.2		0.4	
$(\mathbf{x},\mathbf{y})$	ω	ψ	ω	ψ	ω	ψ
(-0.6,-0.6)	0.0070	0.0014	0.0072	0.0015	0.0079	0.0017
(-0.2,-0.6)	0.0114	0.0023	0.0117	0.0024	0.0128	0.0027
(0.2,-0.6)	0.0114	0.0023	0.0117	0.0024	0.0128	0.0027
(0.6,-0.6)	0.0070	0.0014	0.0072	0.0015	0.0079	0.0017
(-0.6,-0.2)	0.0114	0.0023	0.0117	0.0024	0.0128	0.0027
(-0.2,-0.2)	0.0184	0.0038	0.0189	0.0039	0.0208	0.0044
(0.2,-0.2)	0.0184	0.0038	0.0189	0.0039	0.0208	0.0044
(0.6,-0.2)	0.0114	0.0023	0.0116	0.0024	0.0128	0.0027

Baghdad Science Journal
2022, 19(2): 321-328
P-ISSN: 2078-8665
E-ISSN: 2411-7986

Table 4. Errors bounds: $E_h^n(\psi)$, $E_h^n(\omega)$

n	h	$E_h^n(\psi)$	$E_h^n(\omega)$
100	0.4	0.0024	0.0059
	0.2	6.1250e-04	0.0015
200	0.4	0.0014	0.0044
	0.2	3.3750e-04	0.0011
400	0.4	3.2500e-04	0.0012
	0.2	1.0000e-04	3.1250e-04

Table 5. $\|H_n\|_2 = max_s|\lambda_s|$

n	h	$\|H_n\|_2$
	0.4	0.990436
100	0.2	0.990190
	0.1	0.990128
	0.4	0.990473
200	0.2	0.990233
	0.1	0.990172
	0.4	0.990492
400	0.2	0.990255
	0.1	0.990195

Numerical Simulations

The discrete graphs of vorticity and stream functions (for $h = 0.1$) at time levels $n = 0, 200$ and 400 are presented in Figures 1, 2 and 3, respectively. Clearly, by Figs. 1-3, it is observed that the discrete graphs for vorticity and stream are decreasing as time increases and that supports the numerical results.

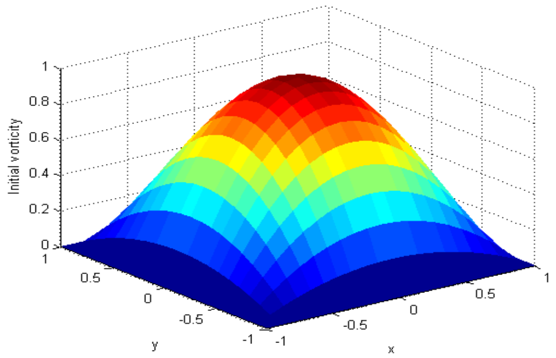

a. Vorticity Graph

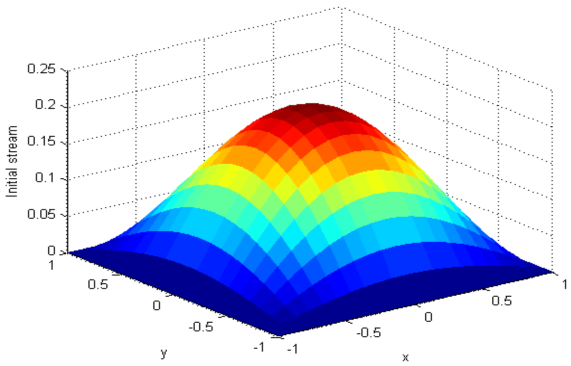

b. Stream Graph
Figure 1. Numerical solutions at $t = 0$

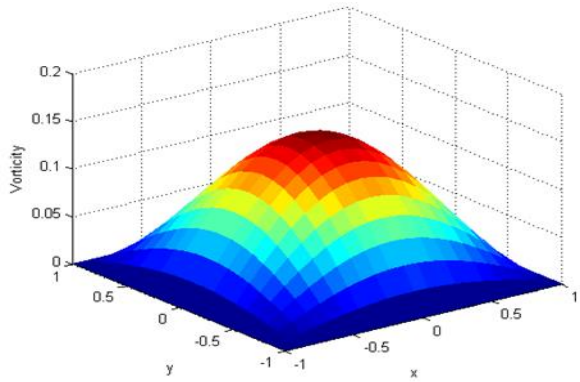

a. Vorticity Graph

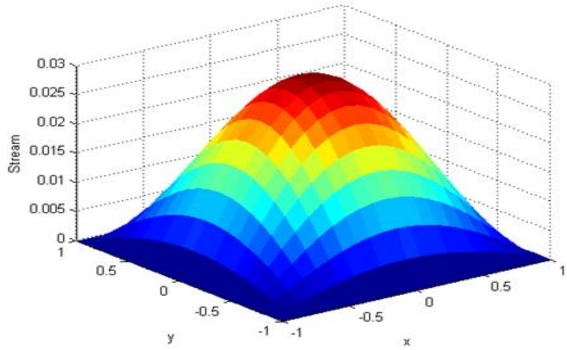

b. Stream Graph
Figure 2. Numerical solutions at $t = 0.4$

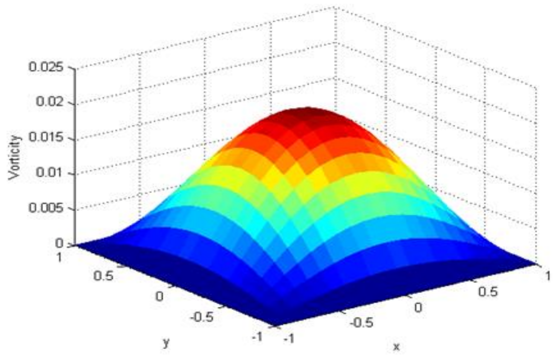

a. Vorticity Graph

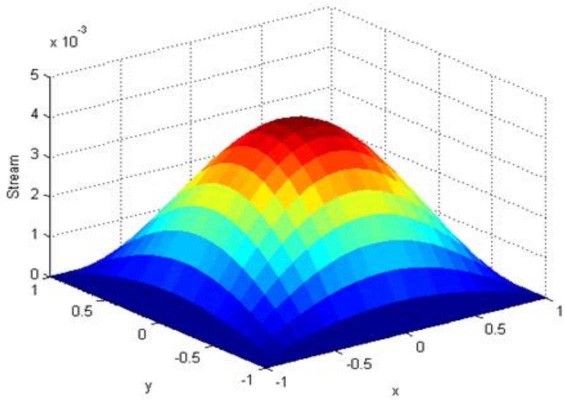

b. Stream Graph
Figure 3. Numerical solutions at $t = 0.8$

Conclusions:

This paper is concerned with the numerical solutions of the vorticity transport equation with homogenous Dirichlet boundary conditions using Crank-Nicolson finite difference scheme. From this work, the following conclusions are pointed out:

1- Crank-Nicolson finite difference scheme is consistent. Moreover, the order of the local truncation error has the form: $O(k^2 + kh^2)$.
2- At a fixed time level, the corresponding error bounds decrease, as the space grids are refined. This indicates that the numerical solution is convergent.
3- At any fixed space-step, the corresponding errors decrease as time increases.
4- Table 5 shows that the numerical results are stable with any space-step and time level.
5- Tables (1- 3) and Figures (1- 3) show that the numerical values for vorticity and stream are decreasing as time level increases.

For future work, the following directions may be considered:

1. Other finite difference schemes can be proposed to find the numerical solution of problem (1)-(4), such as implicit Euler scheme.
2. One could solve problem (1)-(4), with a certain initial function using different consistent finite difference schemes including the present one in order to make a numerical comparison between the results regarding stability and error bounds.
3. With a very large Reynolds number, the nonlinear terms in equation (1) are dominated, so that may affect the stability properties of the proposed scheme. Therefore, in this case, other numerical methods should be adapted to solve the problem.

Acknowledgment:

The authors would like to thank the anonymous reviewers for their remarkable comments and suggestions to improve the present work.

Authors' declaration:

- Conflicts of Interest: None.
- We hereby confirm that all the Figures and Tables in the manuscript are mine ours. Besides, the Figures and images, which are not mine ours, have been given the permission for re-publication attached with the manuscript.
- Ethical Clearance: The project was approved by the local ethical committee in University of Mustansiriyah.

Authors' contributions statement:

The following is a summary of the contribution of each author in the construction of the content of the manuscript

- Maan A. Rasheed: Conceptualized the idea and drafted the concept note. He participated also in the validation of the work and manuscript preparation.
- Suad Naji Kadhim: Participated in the review of literature, running simulations, and drafting the results and discussions.

References:

1. Alabedalhadi M, Al-Smadi M, Al-Omari S, Baleanu D, Momani S. Structure of optical soliton solution for nonlinear resonant space-time Schrödinger equation in conformablesense with full nonlinearity term. Phys. Scr. 2020; 95 (10): 105215.
2. Al-Smadi M, Abu Arqub O. Computational algorithm for solving fredholm time-fractional partial integrodifferential equations of dirichlet functions type with error estimates. Appl. Math. Comput. 2019; 342(C): 280-294.
3. Al-Smadi M, Freihat A, Khalil H, Momani S, Khan R A. Numerical multistep approach for solving fractional partial differential equations. Int. J. Comput. Methods. 2017; 14 (3): 1750029.
4. Al-Smadi M, Abu Arqub O, Momani S. Numerical computations of coupled fractional resonant Schrödinger equations arising in quantum mechanics under conformable fractional derivative sense. Phys. Scr. 2020; 95 (7):075218.
5. Al-Smadi M, Abu Arqub O, Hadid S. An attractive analytical technique for coupled system of fractional partial differential equations in shallow water waves with conformable derivative. Commun. Theor. Phys. 2020; 72 (8): 085001.
6. Tu J, Yeoh GH, Liu C.Computational fluid dynamics: A Practical Approach. 3d edition, Butterworth–Heinemann, UK; 2018.
7. Kaushik A. Numerical study of 2D incompressible flow in a rectangular domain using chorin's projection method at high Reynolds number. Int. j. math. eng. manag. sci. 2019; 4(1): 157–169.
8. Pozrikidis C. Equation of motion and vorticity transport. In: Fluid Dynamics. Springer, Boston, MA; 2017.
9. Speziale C G. On the advantages of the vorticity-velocity formulation of the equations of fluid dynamics. J. Comput. Phys. 1987; 73: 476-480.
10. Tezduyar T E, Liou J, Ganjoo D K, Behr M. Solution techniques for the vorticity-streamfunction formulation of two-dimensional unsteady

11. incompressible flows. Int. J. Numer. Methods Fluids, 1990; 11(5):515–539
12. Dennis SC. The numerical solution of the vorticity transport equation. InProceedings of the third international conference on numerical methods in fluid mechanics 1973 (pp. 120-129). Springer, Berlin, Heidelberg.
13. Joseph M. Finite difference representations of vorticity transport. Comput Methods Appl Mech Eng. 1983 Aug 1;39(2):107-16.
14. Napolitano M , Pascazio G. A numerical method for the vorticity-velocity Navier-Stokes equations in two and three dimensions. Computers & Fluids. 1991 Jan 1;19(3-4):489-95
15. Lo D C. Murugesan K , Young D L. Numerical solution of three-dimensional velocity–vorticity Navier–Stokes equations by finite difference method. Int. J. Numer. Methods Fluids. 2005; 47(12): 1469-1487.
16. Ambethkar V , Kumar M , Srivastava M K. Numerical solutions of 2-d unsteady incompressible flow in a driven square cavity using streamfunction-vorticity formulation. Int. J. Appl. Math. 2016; 29 (6): 727-757.
17. Rasheed M A, Balasim A T, Jameel A F. Some results for the vorticity transport equation by using A.D.I scheme, AIP Conference Proceedings. 2019; 2138, 030031; doi.org/10.1063/1.5121068
18. Ravnik J, Tibaut J. Boundary-domain Integral method For vorticity transport equation with variable viscosity. Int. J. Comp. Meth. and Exp. Meas. 2018; 6(6): 1087–1096.
19. Mitchell A R. Computational methods in partial differential equations, Wiley, London; 1969.

الحلول العددية لمعادلة نقل الحركة الدورانية ثنائية الأبعاد باستخدام طريقة كرانك-نيكلسون

معن عبد الكاظم رشيد [1] سعاد ناجي كاظم [2]

[1] قسم الرياضيات، كلية التربية الاساسية، الجامعة المستنصرية، بغداد ، العراق
[2] قسم الرياضيات، كلية العلوم، جامعة بغداد، بغداد، العراق

الخلاصة:

يهتم هذا البحث بالحلول العددية لمعادلة نقل الحركة الدوارنية (VTE) ثنائية الابعاد مع شروط ديرشلت الحدودية المتجانسة . وبالتحديد، نشتق معادلة الفروقات المنتهية (Crank-Nicolson) لهذه المسألة. بالإضافة إلى ذلك، نناقش اتساق واستقرار الطريقة. علاوة على ذلك، يتم التطرق الى تجربة عددية لدراسة تقارب طريقة (Crank-Nicolson) ولتصور الرسوم البيانية المتقطعة لكلا من دوال الحركة الدورانية والتدفق. تظهر النتيجة النظرية أن الطريقة المقترحة متسقة، في حين أن النتائج العددية تظهر أن الحلول مستقرة عند خطوات مساحة صغيرة وفي أي مستويات زمنية.

الكلمات المفتاحية: الفروقات المنتهية، عدد رينولد، دالة التدفق، خطأ القطع، دالة الحركة الدوانية.